Science of the Total Environment 927 (2024) 172306

Contents lists available at ScienceDirect

Science of the Total Environment

journal homepage: www.elsevier.com/locate/scitotenv

Comparison of intestinal toxicity in enhancing intestinal permeability and in causing ROS production of six PPD quinones in *Caenorhabditis elegans*

Yuxing Wang [a], Geyu Liang [b], Jie Chao [a], Dayong Wang [a,c,*]

[a] Key Laboratory of Environmental Medicine Engineering of Ministry of Education, Medical School, Southeast University, Nanjing, China
[b] School of Public Health, Southeast University, Nanjing, China
[c] Shenzhen Ruipuxun Academy for Stem Cell & Regenerative Medicine, Shenzhen, China

HIGHLIGHTS

- PPDQs could enhance intestinal permeability of nematodes to different degrees.
- PPDQs caused oxidative stress associated with enhanced intestinal permeability.
- 77PDQ could induce more severe intestinal toxicity than other PPDQs.
- IPPDQ showed the lowest intestinal toxicity compared to other PPDQs.

GRAPHICAL ABSTRACT

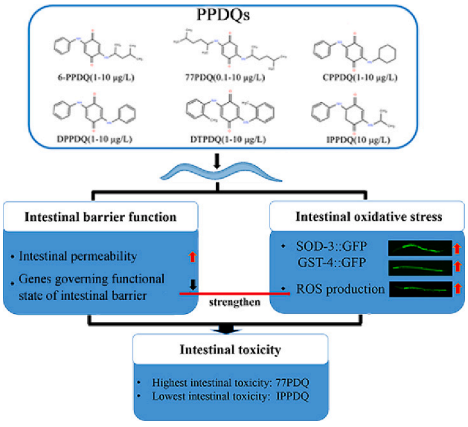

ARTICLE INFO

Editor: Daqiang Yin

Keywords:
C. elegans
Intestinal toxicity
Toxicity comparison
PPDQs

ABSTRACT

As the derivatives of *p*-phenylenediamines (PPDs), PPD quinones (PPDQs) have received increasing attention due to their possible exposure risk. We compared the intestinal toxicity of six PPDQs (6-PPDQ, 77PDQ, CPPDQ, DPPDQ, DTPDQ and IPPDQ) in *Caenorhabditis elegans*. In the range of 0.01–10 μg/L, only 77PDQ (10 μg/L) moderately induced the lethality. All the examined PPDQs at 0.01–10 μg/L did not affect intestinal morphology. Different from this, exposure to 6-PPDQ (1–10 μg/L), 77PDQ (0.1–10 μg/L), CPPDQ (1–10 μg/L), DPPDQ (1–10 μg/L), DTPDQ (1–10 μg/L), and IPPDQ (10 μg/L) enhanced intestinal permeability to different degrees. Meanwhile, exposure to 6-PPDQ (0.1–10 μg/L), 77PDQ (0.01–10 μg/L), CPPDQ (0.1–10 μg/L), DPPDQ (0.1–10 μg/L), DTPDQ (1–10 μg/L), and IPPDQ (1–10 μg/L) resulted in intestinal reactive oxygen species (ROS) production and activation of both SOD-3::GFP and GST-4::GFP. In 6-PPDQ, 77PDQ, CPPDQ, DPPDQ, DTPDQ, and/or IPPDQ exposed nematodes, the ROS production was strengthened by RNAi of genes (*acs-22*, *erm-1*, *hmp-2*, and *pkc-3*) governing functional state of intestinal barrier. Additionally, expressions of *acs-22*, *erm-1*, *hmp-2*, and *pkc-3* were negatively correlated with intestinal ROS production in nematodes exposed to 6-PPDQ, 77PDQ, CPPDQ, DPPDQ, DTPDQ, and/or IPPDQ. Therefore, exposure to different PPDQs differentially induced the intestinal toxicity on

* Corresponding author at: Key Laboratory of Environmental Medicine Engineering of Ministry of Education, Medical School, Southeast University, Nanjing, China.
E-mail address: dayongw@seu.edu.cn (D. Wang).

https://doi.org/10.1016/j.scitotenv.2024.172306
Received 20 February 2024; Received in revised form 3 April 2024; Accepted 5 April 2024
Available online 7 April 2024

nematodes. Our data highlighted potential exposure risk of PPDQs at low concentrations to organisms by inducing intestinal toxicity.

1. Introduction

Some *p*-phenylenediamines (PPDs) are used as antiozonants and antioxidants in rubber tires to inhibit their oxidative degradation (Seiwert et al., 2022). Due to abrasion of rubber tire on road surface, PPDs will enter urban environment together with tire wear particles (Deng et al., 2022). In the environment, after ozonation, PPDs can be transformed to PPD quinones (PPDQs) through different chemical pathways, including *N*-1,3-dimethylbutyl-*N*-phenyl quinone diamine (QDI), intermediate phenol, and semiquinone radical pathways (Hua and Wang, 2023a). N-(1,3-dimethylbutyl)-*N*′-phenyl-*p*-phenylenediamine (6-PPD) is a representative of PPDs, and its transformative product after ozonation is 6-PPDQ (Tian et al., 2021). 6-PPDQ was the mainly detected PPDQ in various environments, including urban runoff, wastewater, road dusts, soil, and sediment (Cao et al., 2022; Johannessen and Metcalfe, 2022; Zeng et al., 2023; Maurer et al., 2023). Besides 6-PPD, some other PPDs were also detected in the environment. DPPD, and DTPD could be detected in water from Zhujiang River and Dongjiang River (Zhang et al., 2023b). CPPD was detected in water and sediment (Zhu et al., 2024a; Zhu et al., 2024b). 77PDQ was detected in urban rivers and $PM_{2.5}$ (Wang et al., 2022; Zeng et al., 2023). IPPDQ was detected in wastewater and sediment (Jin et al., 2023; Cao et al., 2023). These observations have implied the possible exposure risk of PPDQs in the environments.

After the identification of 6-PPDQ as cause of acute mortality of coho salmon, some other aspects of 6-PPDQ toxicities have been reported. In zebrafish, 6-PPDQ exposure induced intestinal lesions, cardiotoxicity, and induction of some abnormal behaviors (Zhang et al., 2023a; Ji et al., 2022a; Varshney et al., 2022). The increased oxygen consumption was also observed in embryo of zebrafish or rainbow trout gill cells (Varshney et al., 2022; Mahoney et al., 2022). Damage on multiple organs including lung, liver, and kidney could be observed in male mice after repeated exposure (Fang et al., 2023; He et al., 2023a; He et al., 2024). Accompanied with the observed toxicity, 6-PPDQ was accumulated in fish samples and different organs of mice (Ji et al., 2022b; Grasse et al., 2023; He et al., 2023a).

Caenorhabditis elegans is an important animal model for performing toxicity assessment of pollutants because of its easy maintenance, small size, and short life-cycle (Wang, 2020; Liu et al., 2023; Zhuang et al., 2024). In addition, considering the sensitivity to environmental exposure (Wang, 2022; Wang et al., 2019; Yu et al., 2023), *C. elegans* can be used to detect toxicity of pollutants at environmentally relevant concentrations (Tang et al., 2023; Wang et al., 2023c; He et al., 2023b). In *C. elegans*, exposure to 6-PPDQ (1–10 μg/L) induced reduction in reproductive capacity mediated by germline apoptosis and caused behavioral abnormality partially associated with neurodegeneration (Hua et al., 2023a; Hua et al., 2023b; Hua and Wang, 2024). Additionally, exposure to 6-PPDQ (1-10 μg/L) reduced both lifespan and health span of nematodes (Hua and Wang, 2023c). Lipid and dopamine metabolisms could be further disrupted by exposure to 6-PPDQ (1–10 μg/L) in nematodes (Hua and Wang, 2023b; Wang et al., 2023a). Meanwhile, 6-PPPQ accumulation was detected in 1–10 μg/L 6-PPDQ exposed nematodes (Hua and Wang, 2023c).

So far, some reports have described accumulation and toxicity of 6-PPDQ in different organisms (Chen et al., 2023; Hua and Wang, 2023a). In contrast to this, little is known about the behavior of other PPDQs in organisms. We assumed that different PPDQs may cause different toxic effects on organisms. In *C. elegans*, damage on secondary targeted organs (such as neurons and gonad) was largely due to the damage on intestinal barrier, the primary targeted organs (Wang, 2019). Intestinal oxidative stress and enhanced intestinal permeability were detected in 1–10 μg/L 6-PPDQ exposed nematodes (Hua et al., 2023c). Thus, using *C. elegans* as animal model, we here compared intestinal toxicity of PPDQs, including the 6-PPDQ, 77PDQ, CPPDQ, DPPDQ, DTPDQ and IPPDQ. The environmental concentrations of PPDQs are in the range from ng/L to μg/L (Wang et al., 2022; Zhao et al., 2023; Zeng et al., 2023; Zhu et al., 2024a, 2024b). We focused on assessment of intestinal toxicity in nematodes exposed to PPDQs in the range of ng/L and μg/L. Our results indicated that, besides 6-PPDQ, some other PPDQs also need the attention for their possible exposure risk to and toxic effect on environmental organisms.

2. Materials and methods

2.1. Reagents

6-PPDQ was purchased from Toronto Research Chemicals Co., Toronto, Canada (catalogue: P348790). The 77PDQ (catalogue: SCAH-101024), CPPDQ (catalogue: IST175530), DPPDQ (catalogue: SCAH-101012), DTPDQ (catalogue: IST175532), and IPPDQ (catalogue: IST171264) were purchased from Shanghai SCR-Biotech Co., Ltd., Shanghai, China. Purities of 6-PPDQ, 77PDQ, CPPDQ, DPPDQ, DTPDQ and IPPDQ were > 97 %, >98 %, >98 %, >98 %, >98 % and > 98 %, respectively. All the examined PPDQs were dissolved in dimethyl sulfoxide (DMSO) , and the concentration of stocking solution was 1 g/L. Working solutions for PPDQs (0.01–10 μg/L) were prepared after dilution with K buffer. The control solution was prepared by diluting DMSO with K buffer, and the dilution method was the same as that of PPDQs solution. To avoid the adverse effects of DMSO on nematodes, the final DMSO concentration was equal to 0.1 % (González-Manzano et al., 2012).

The 6-PPDQ is composed of p-benzoquinone, phenyl, and 1,3-dimethylbutyl (Fig. 1A). Compared to 6-PPDQ, 77PDQ consists of p-benzoquinone and two 1,4-dimethylpentyl groups (Fig. 1A), CPPDQ is composed of p-benzoquinone, phenyl, and cyclohexyl (Fig. 1A), DPPDQ consists of p-benzoquinone and two phenyl groups (Fig. 1A), DTPDQ consists of p-benzoquinone and two ortho-methylphenyl groups (Fig. 1A), and IPPDQ consists of p-benzoquinone-like structure (product of olefin hydrogenation coupled with aniline on the 5-position carbon atom of the p-benzoquinone skeleton), phenyl, and isopropyl (Fig. 1A).

2.2. Animal maintenance

The information of *C. elegans* strains used is shown in Table S1. According to standard protocol, *C. elegans* is cultured on nematode growth medium (NGM) supplemented with *E. coli* OP50 as a food source (Brenner, 1974). The wild-type strain was N2. To obtain synchronized spawning from gravid hermaphrodite adults, a bleach solution (2 % HOCl, 0.45 M NaOH) was utilized (Wang et al., 2023b). To obtain sufficient L1 larvae, the collected eggs were transferred onto a new NGM plate and allowed to hatch and develop to the L1-larval stage at a temperature of 20 °C (Shao et al., 2023).

2.3. Exposure

Exposure to PPDQs was started from L1 larvae until the stage of adult day-1 (approximately for 4.5 days) (Hua et al., 2023c). L1 larval precipitate was dispensed into each concentration of PPDQs solution and concentrated OP50 was added. Each exposure group contained 600 μL exposure solution and approximately 300 animals. Fresh exposure solutions were replaced every day during exposure process.

2.4. Lethality

Lethality can be reflected by the percentage of surviving nematodes (Wang, 2020). After exposure, the number of dead nematodes was counted under a dissecting microscope, and dead nematodes were verified by failing to respond to stimulation of inactive nematodes with a metallic platinum wire. One hundred nematodes were examined for each exposure group. The experiment was performed in triplicate.

2.5. Intestinal permeability analysis

After PPDQs exposure and washing three times with M9 buffer, the nematodes were stained by 5.0 % erioglaucine disodium for 3 h in the darkness (Hua et al., 2023c). After staining, the animals were further washed by K buffer until the liquid becomes colorless and transparent. The images were captured using bright field of microscopy. Fifty animals were analyzed for each exposure. Under the normal condition, the blue signals are mainly located in intestinal lumen. Once the intestinal barrier is disrupted, the blue signals would be detected in intestinal cells and even in body cavity.

2.6. Reactive oxygen species (ROS) assay

In nematodes, levels of intestinal ROS can be used to reflect the induction of oxidative stress (Wang, 2020). After exposure, the tested animals were washed three times. Then, 1 μM CM-H_2DCFDA was used to label *C. elegans* ROS for 3 h in darkness. After washing three times using K buffer, the animals were transferred onto 2 % agarose pad. Intestinal fluorescent signals in nematodes were detected using laser confocal microscope under the FITC signaling pathway (excitation/emission wavelengths: 488/510 nm). After normalization to intestinal auto-fluorescence, intensity of intestinal ROS signals was semi-quantified using Image J software. Fifty animals were analyzed for each exposure.

2.7. SOD-3::GFP and GST-4::GFP expressions

The used transgenic strains were CF1533 (SOD-3::GFP) and CL2166 (GST-4::GFP). These transgenic strains can be used as indicators of activation of oxidative stress caused by exposure to some pollutants. (Wang, 2019). SOD-3 and GST-4 can be expressed in intestine. Relative fluorescence intensity of intestinal SOD-3::GFP and GST-4::GFP signals were examined. For each exposure, 50 animals were analyzed.

2.8. Transcriptional expression analysis

Total RNA was extracted using Trizol. RNA quality was determined based on OD260/280 ratio in Nanodrop One. Quantitative real-time polymerase chain reaction (qRT-PCR) was carried out in ABI 7500

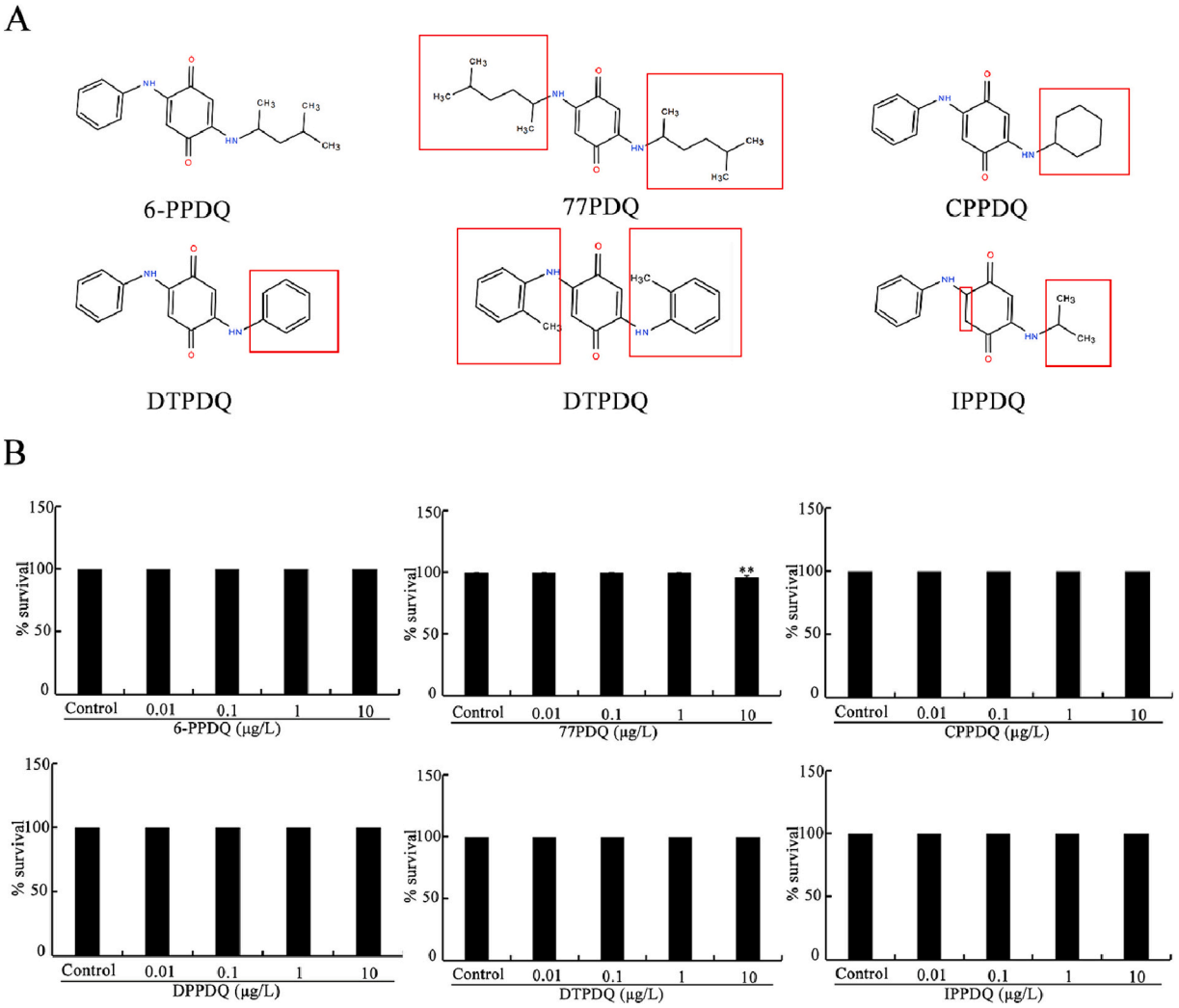

Fig. 1. Toxicity comparison of PPDQs in inducing lethality. (A) Chemical structures of 6-PPDQ, 77PDQ, CPPDQ, DPPDQ, DTPDQ, and IPPDQ. (B) Effect of exposure to 6-PPDQ, 77PDQ, CPPDQ, DPPDQ, DTPDQ and IPPDQ on survival of nematodes. $^{**}P < 0.01$ vs control.

PCR system using SYBR Green master mix for detection of targeted gene. Comparative cycle threshold method was applied to normalize expression of target gene with reference gene (*tba-1*) (Hua et al., 2023d). Experiment was performed in triplicate. Primers are shown in Table S1.

2.9. RNA interference (RNAi)

Gene constructs for RNAi were generated in L4440, an empty vector, and subsequently transformed into *E. coli.* HT115 (Shao et al., 2024). Before experiment, RNAi were cultured on NGM plates containing 1 mM isopropylthiogalactoside for 24 h to induce double-stranded RNA. Nematodes were fed with RNAi, and the progeny were used for exposure to PPDQs. The control consisted of HT115 expressing L4440 (Liu et al., 2024). qRT-PCR was carried out to assess RNAi efficiency (Fig. S1).

2.10. Correlation analysis

Correlations between expression of genes controlling intestinal barrier function and ROS production by PPDQs exposure were assessed using Pearson correlation analysis. Relative gene expression and relative fluorescence intensity of ROS production were analyzed by correlation matrix in multivariate analysis on GrashPad Prism 8 software. Pearson's correlation coefficient r and the *p*-value were calculated. The correlation heatmap was then plotted by the pheatmap package on R Studio.

2.11. Analysis of GSH and MDA

GSH (L-glutathione) and MDA (malonydialdehyde) are also indicators for oxidative stress activation, and were analyzed using corresponding kits purchased from Nanjing Jiangcheng Bioengineering Institute (Nanjing, China) and Sangon Biotech (Shanghai) Co. For GSH assay, according to the manufacturer's protocol in total glutathione/oxidized glutathione assay kit, the supernatants prepared as indicated above were mixed the reagents and standard sample of GSH. The resulting mixture was then measured for the absorbance at 405 nm using spectrophotometer. Three independent experiments were performed. For MDA assay, according to the manufacturer's protocol in malondialdehyde assay kit, the lysates after homogenization in liquid nitrogen was mixed with a specific reagent provided by the kit. After water bath for 10 min, samples were centrifuged at 3500 rpm for 10 min. The supernatants were measured for their absorbance at 532 nm spectrophotometer. Three independent experiments were performed.

2.12. Data analysis

Using SPSS Statistics 25.0, statistical differences between different groups were evaluated by analysis of variance (ANOVA). Statistical significance was defined as a probability level of 0.01.

3. Results

3.1. Toxicity comparison of PPDQs in inducing lethality

All the examined PPDQs at 0.01–1 μg/L did not induce lethality (Fig. 1B). Additionally, exposure to 6-PPDQ, CPPDQ, DPPDQ, DTPDQ and IPPDQ at 10 μg/L also did not induce lethality (Fig. 1B). Only exposure to 77PDQ (10 μg/L) could cause obvious lethality in nematodes (Fig. 1B). In 77PDQ (10 μg/L) exposed nematodes, approximately 4 % nematodes showed lethality.

3.2. Effect of PPDQs on intestinal morphology

Considering the important role of intestinal barrier in defending against toxicity of pollutants (Wang, 2019), we next examined effects of PPDQs on intestinal morphology. All the examined 6 PPDQs at 0.01–10 μg/L could not affect morphology and width of intestinal lumen (Fig. S2). Therefore, PPDQs exposure at 0.01–10 μg/L may not cause severe adverse effects on intestinal development in nematodes.

3.3. Toxicity comparison of PPDQs in affecting intestinal permeability

To investigate effect of PPDQs on functional state of intestinal barrier, we used blue dye (erioglaucine disodium) to evaluate intestinal permeability. Blue signals tend to accumulate within the lumen of intestines under the normal condition (Fig. 2A). Exposure to all PPDQs at 0.01 μg/L, as well as 6-PPDQ, CPPDQ, DPPDQ, DTPDQ, and IPPDQ at 0.1 μg/L, did not result in any alteration in the positioning of blue signals within the intestinal lumen (Fig. 2A). However, exposure to 6-PPDQ (1 μg/L), 77PDQ (0.1 μg/L), CPPDQ (1 μg/L), DPPDQ (1 μg/L), DTPDQ (1–10 μg/L), and IPPDQ (10 μg/L) could induce the translocation and accumulation of blue dye from the intestinal lumen to intestinal cells (Fig. 2A). Additionally, exposure to 6-PPDQ (10 μg/L), 77PDQ (1–10 μg/L), CPPDQ (10 μg/L), and DPPDQ (10 μg/L) could further cause translocation and accumulation of blue dye not only within intestinal cells but also within body cavity (Fig. 2A).

In nematodes, ACS-22, ERM-1, PKC-3, HMP-2, and ACT-5 are required for regulation of functional state of intestinal barrier (Ren et al., 2018; Liu et al., 2019; Wang, 2019). Exposure to 6PPDQ, CPPDQ, DPPDQ, DTPDQ, and IPPDQ at the concentration of 0.01–0.1 μg/L did not influence *act-5*, *acs-22*, *erm-1*, *hmp-2*, and *pkc-3* expressions (Fig. 2B). Among the examined 5 genes, exposure to 6PPDQ at concentrations of 1 and 10 μg/L only decreased *acs-22* expression (Fig. 2B). Among the examined genes, 0.01 μg/L 77PDQ only decreased *hmp-2* expression, 0.1 μg/L 77PDQ decreased *hmp-2* and *pck-3* expressions, 1 μg/L 77PDQ decreased *acs-22*, *hmp-2*, and *pkc-3* expressions, and 10 μg/L 77PDQ decreased *acs-22*, *erm-1*, *hmp-2*, and *pkc-3* expressions (Fig. 2B). After the exposure, 1 μg/L CPPDQ only decreased *hmp-2* expression, and 10 μg/L CPPDQ could decrease *acs-22* and *hmp-2* expressions (Fig. 2B). Exposure to DPPDQ (1–10 μg/L) notably decreased *acs-22* and *pkc-3* expressions (Fig. 2B). Exposure to 1 μg/L DTPDQ decreased *pkc-3* expression, and 10 μg/L DTPDQ decreased *pkc-3* and *hmp-2* expressions (Fig. 2B). The decrease in expressions of *pkc-3* and *acs-22* was also observed in 10 μg/L IPPDQ exposed nematodes (Fig. 2B).

3.4. Toxicity comparison of PPDQs in inducing intestinal ROS production

Next, we used ROS production as endpoint to detect intestinal oxidative stress response to PPDQs. Exposure to 6-PPDQ (0.01 μg/L), CPPDQ (0.01 μg/L), DPPDQ (0.01 μg/L), DTPDQ (0.01 and 0.1 μg/L), and IPPDQ (0.01 and 0.1 μg/L) did not induce ROS production (Fig. 3). Different from these, exposure to 6-PPDQ (0.1–10 μg/L), 77PDQ (0.01–10 μg/L), CPPDQ (0.1–10 μg/L), DPPDQ (0.1–10 μg/L), DTPDQ (1–10 μg/L), and IPPDQ (1–10 μg/L) resulted in significant induction of intestinal ROS production (Fig. 3).

Moreover, MDA content was significantly increased by 0.1–10 μg/L 6-PPDQ, 0.01–10 μg/L 77PDQ, 0.1–10 μg/L CPPDQ, 0.1–10 μg/L DPPDQ, 1–10 μg/L DTPDQ, and 1–10 μg/L IPPDQ (Fig. S3A). In contrast, GSH content was significantly decreased in 0.1–10 μg/L 6-PPDQ, 0.01–10 μg/L 77PDQ, 0.1–10 μg/L CPPDQ, 0.1–10 μg/L DPPDQ, 1–10 μg/L DTPDQ, and 1–10 μg/L IPPDQ exposed nematodes (Fig. S3B).

3.5. Comparison of effect of PPDQs on expressions of SOD-3::GFP and GST-4::GFP

Besides the ROS production, we also examined the effect of exposure to PPDQs (0.01–10 μg/L) on SOD-3::GFP and GST-4::GFP expressions. Exposure to 0.01 μg/L 6-PPDQ, 0.01 μg/L CPPDQ, 0.01 μg/L DPPDQ, 0.01–0.1 μg/L DTPDQ, and 0.01–0.1 μg/L IPPDQ did not cause alteration in expressions of SOD-3::GFP and GST-4::GFP (Fig. 4A and B). Different from these, expressions of SOD-3:: GFP and GST-4:: GFP were

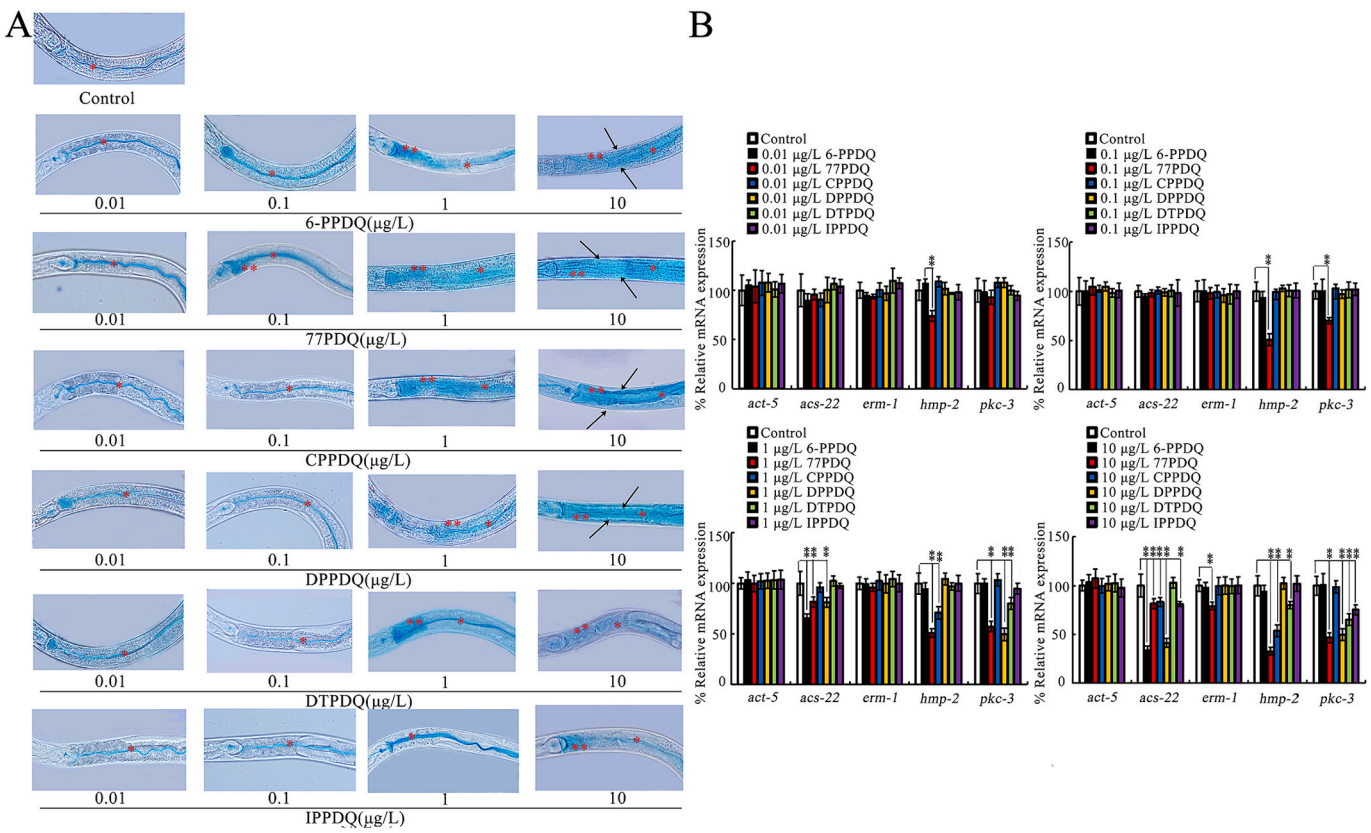

Fig. 2. Toxicity comparison of PPDQs in enhancing intestinal permeability (A) and affecting intestinal expression of genes governing functional state of intestinal barrier (B). The intestinal cells (**) and intestinal lumen (*) were labeled by asterisks, and the body cavity was labeled by arrowheads. For qRT-PCR analysis, 30 intact intestines were subjected to RNA extraction. $^{**}P < 0.01$.

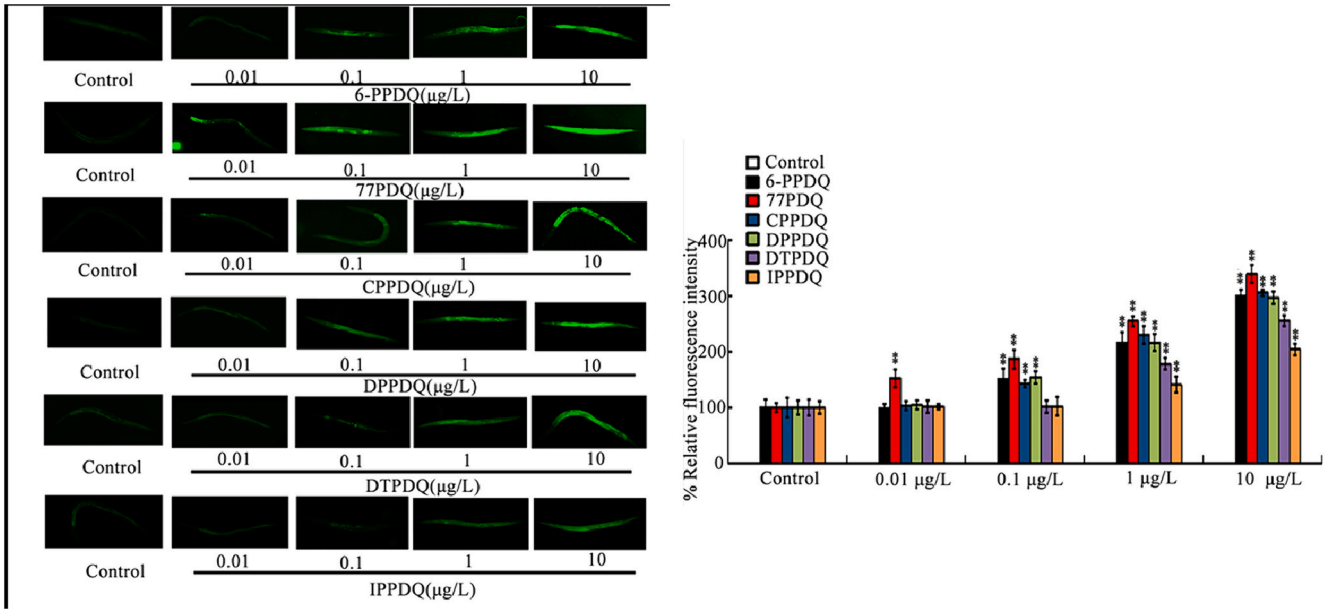

Fig. 3. Toxicity comparison of PPDQs on induction of intestinal ROS production. $^{**}P < 0.01$ vs control.

increased in 6-PPDQ (0.1–10 μg/L), 77PDQ (0.01–10 μg/L), CPPDQ (0.1–10 μg/L), DPPDQ (0.1–10 μg/L), DTPDQ (1–10 μg/L), and IPPDQ (1–10 μg/L) exposed nematodes (Fig. 4A and B).

3.6. RNAi of acs-22, erm-1, hmp-2, and pkc-3 affected ROS production in some PPDQs exposed nematodes

Corresponding to the altered genes regulating functional state of intestinal barrier by PPDQs, we further determined the effect of intestinal RNAi of *acs-22*, *erm-1*, *hmp-2*, and *pkc-3* on ROS production in

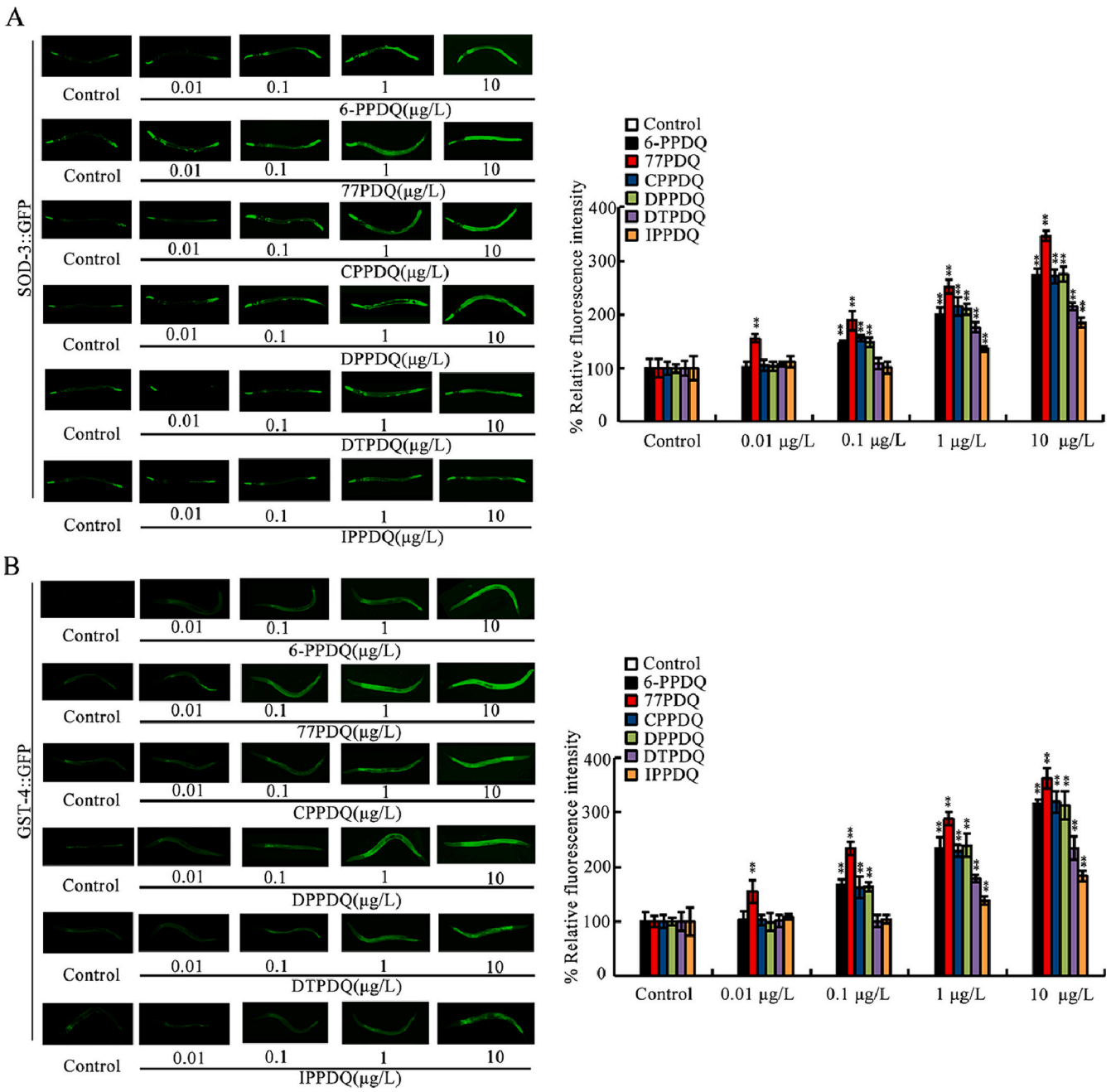

Fig. 4. Comparison of effect of PPDQs on expressions of SOD-3::GFP expression (A) and GST-4::GFP expression (B). $^{**}P < 0.01$ vs control.

PPDQ exposed nematodes using VP303 as tool for intestine-specific RNAi of genes (Hua et al., 2023e). Under normal condition, intestinal RNAi of these genes did not cause oxidative stress in VP303 animals (Fig. 5). In 6-PPDQ exposure group, *acs-22(RNAi)* nematodes showed more severe ROS production compared to VP303 (Fig. 5). In 77PDQ exposure group, *acs-22(RNAi)*, *erm-1(RNAi)*, *hmp-2(RNAi)*, and *pkc-3 (RNAi)* nematodes showed more severe ROS production than VP303 (Fig. 5). After CPPDQ exposure, the more severe ROS production was detected in *hmp-2(RNAi)* and *pck-3(RNAi)* nematodes compared to VP303 nematodes (Fig. 5). After exposure to DPPDQ, RNAi of *acs-22* and *pkc-3* caused more severe ROS production compared to VP303 nematodes (Fig. 5). Meanwhile, we observed more severe ROS production in DTPDQ exposed *hmp-2(RNAi)* and *pkc-3(RNAi)* nematodes compared to that in DTPDQ exposed VP303 nematodes (Fig. 5). In IPPDQ exposed VP303 nematodes, RNAi of *pkc-3* and *acs-22* resulted in more pronounced increase in ROS production compared to VP303 (Fig. 5).

3.7. Expressions of genes regulating functional state of intestinal barrier was correlated with induction of ROS production in PPDQs exposed nematodes

Moreover, we analyzed the possible correlations between expression of genes regulating functional state of intestinal barrier and ROS production in PPDQs exposed nematodes. The *acs-22* expression ($r = -0.957$, $P = 0.011$) showed significant negative correlation with ROS production in 6PPDQ exposed nematodes (Fig. 6). The expressions of *acs-22* ($r = -0.907$, $P = 0.037$), *erm-1* ($r = -0.888$, $P = 0.044$), *hmp-2* ($r = -0.923$, $P = 0.025$), and *pkc-3* ($r = -0.964$, $P = 0.008$) showed significant negative correlation with ROS production in 77PDQ exposed nematodes (Fig. 6). The expressions of gene *acs-22* ($r = -0.919$, $P = 0.027$) and *hmp-2* ($r = -0.983$, $P = 0.003$) exhibited significant negative correlation with ROS production in CPPDQ exposed nematodes (Fig. 6). The expressions of *acs-22* ($r = -0.946$, $P = 0.015$) and *pkc-3* ($r =$

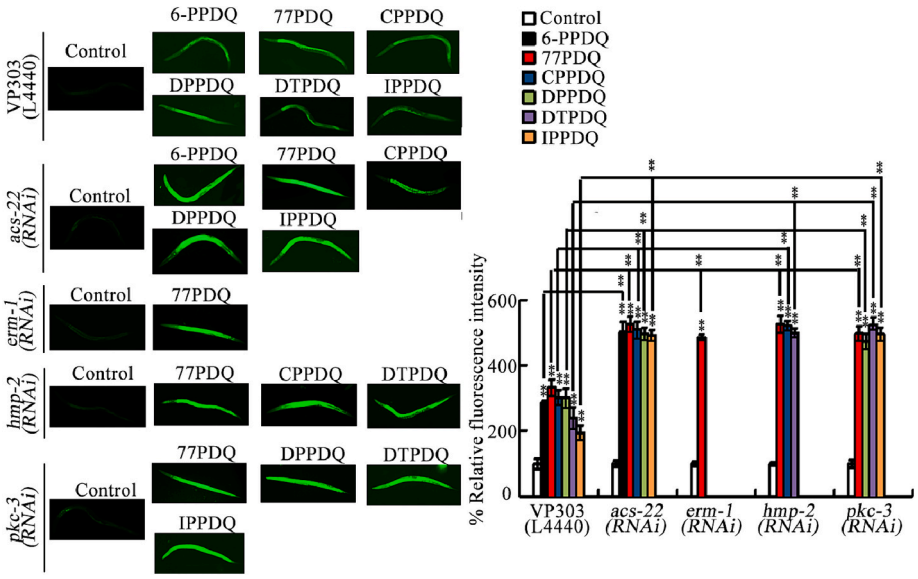

Fig. 5. Effect of RNAi of *acs-22*, *erm-1*, *hmp-2*, or *pkc-3* on intestinal ROS production in PPDQs exposed nematodes. Exposure concentration of PPDQs was 10 μg/L. $^{**}P < 0.01$ vs control (if not specially indicated).

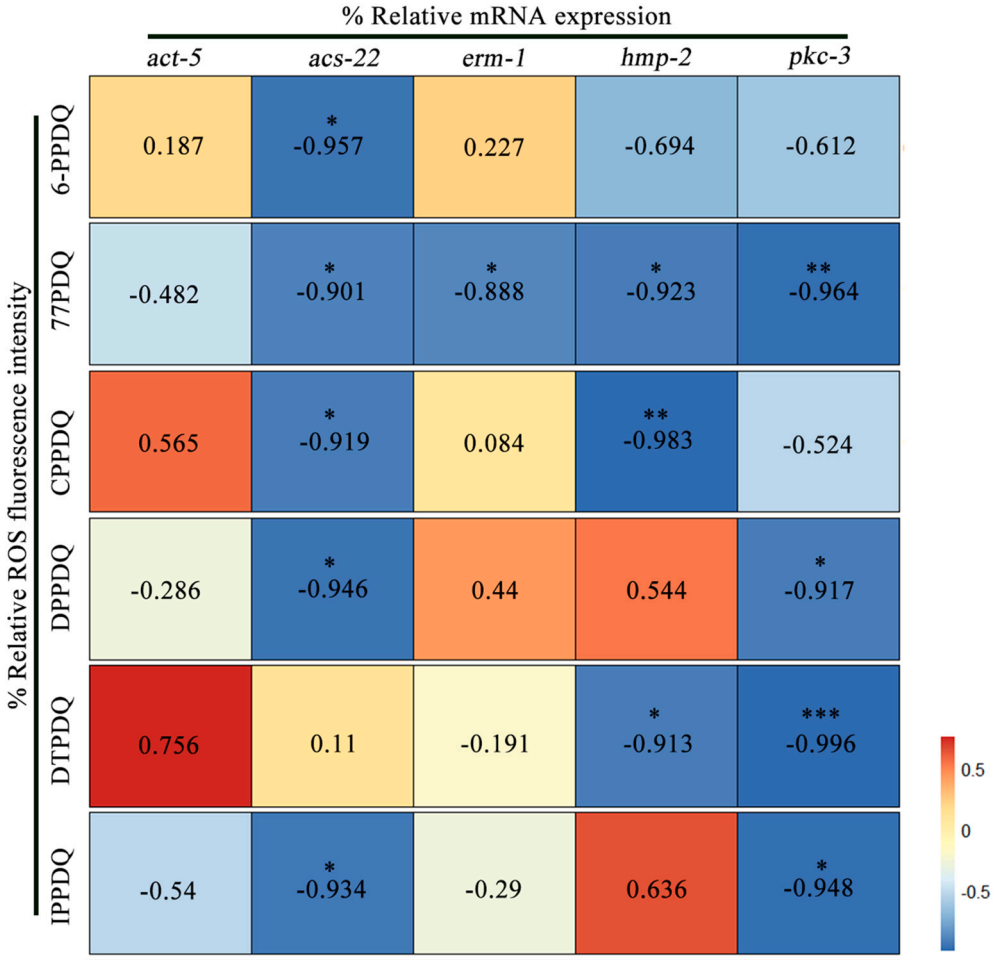

Fig. 6. Correlation analysis between expression of genes required for control intestinal barrier function and induction of ROS production in PPDQs exposed nematodes. *P* represents the significance of the correlation between the two variables. $^{*}P < 0.05$, $^{**}P < 0.01$, and $^{***}P < 0.001$.

−0.917, $P = 0.028$) showed significant negative correlation with ROS production in DPPDQ exposed nematodes (Fig. 6). The expressions of *hmp-2* ($r = -0.913$, $P = 0.031$) and *pkc-3* ($r = -0.996$, $P = 0.0003$) showed significant negative correlation with ROS production in DTPDQ exposed nematodes (Fig. 6). The expressions of *acs-22* ($r = -0.934$, $P = 0.019$) and *pkc-3* ($r = -0.948$, $P = 0.014$) exhibited significant negative correlation with ROS production in IPPDQ exposed nematodes (Fig. 6).

4. Discussion

In the environment, the presence of PPDQs has been commonly observed in urban rivers (Zhang et al., 2023b), air particles (Wang et al., 2022; Cao et al., 2022), dust (Huang et al., 2021), and sediment (Zeng et al., 2023). Some reported environmental concentrations of 6-PPDQ, CPPDQ, DPPDQ, DTPDQ, and IPPDQ in runoff water were 19 μg/L, 200 ng/L, 0.82 ng/L, 360 ng/L, and 560 ng/L, respectively, and the median concentration of 77PDQ reached 527 pg/m^3 in $PM_{2.5}$ from Guangzhou (Tian et al., 2021; Wang et al., 2022; Cao et al., 2022; Zeng et al., 2023; Zhao et al., 2023; Monaghan et al., 2023). These suggests the possible bioavailability of PPDQs to organisms in the environment. Recently, some of the PPDQs have been found in some human urine samples (Mao et al., 2024), which further confirmed this. Although several aspects of 6-PPDQ toxicity on organisms have been described (Hua and Wang, 2023a; Chen et al., 2023), the toxicity of other PPDQs on animals is still largely unknown. Given the high sensitivity to toxicity of environmental contaminants (Wang, 2020; Wang, 2022), in this study, the toxicity of six examined PPDQs was compared in *C. elegans*. Intestinal barrier is normally the primary targeted organ for environmental pollutants (Wang, 2019). Therefore, we focused on the comparison of intestinal toxicity of examined PPDQs in nematodes.

In nematodes, some pollutants (such as nanoplastics) and stresses (such as microgravity stress) could result in the enhancement on intestinal permeability (Liu et al., 2019; Qu et al., 2018). After the exposure, the examined six PPDQs at 0.01–10 μg/L did not influence intestinal morphology (Fig. S1) (Hua et al., 2023c). Different from this, the functional state of intestinal barrier was disrupted by the examined PPDQs to different degrees. Exposure to 77PDQ even at 0.1 μg/L could cause obviously enhanced intestinal permeability (Fig. 2A). Following the 77PDQ, the 6-PPDQ, CPPDQ, DPPDQ, and DTPDQ at 1 and 10 μg/L also caused enhanced intestinal permeability (Fig. 2A). The IPPDQ showed the lowest toxicity on intestinal barrier function, and the enhanced intestinal permeability was only detected in 10 μg/L IPPDQ exposed nematodes (Fig. 2A). The enhancement in intestinal permeability in PPDQs exposed nematodes was reflected by two aspects, dye translocation from intestinal lumen to intestinal cells and dye translocation from intestinal cells further to body cavity (Fig. 2A). The dye translocation from intestinal cells further to body cavity was only observed in 6-PPDQ (10 μg/L), 77PDQ (1–10 μg/L), CPPDQ (10 μg/L), and DPPDQ (10 μg/L) exposed nematodes (Fig. 2A), suggested that 6-PPDQ, 77PDQ, CPPDQ, and DPPDQ exhibited more severe toxicity on intestinal barrier function than DTPDQ and IPPDQ.

In nematodes, intestinal barrier function is under the control of some genes, such as *act-5*, *acs-22*, *erm-1*, *hmp-2*, and *pkc-3* (Liu et al., 2019; Ren et al., 2018; Wang, 2019). Under the normal condition, the intestinal permeability was affected by mutation or RNAi of *act-5*, *acs-22*, *erm-1*, *hmp-2*, and *pkc-3* (Qu et al., 2018; Ren et al., 2018; Liu et al., 2019). Accompanied with the enhanced intestinal permeability, expressions of *acs-22*, *erm-1*, *hmp-2*, and *pkc-3* were decreased by PPDQs to different degree (Fig. 2B). Exposure to 77PDQ at 0.1 μg/L decreased intestinal *hmp-2* and *pkc-3* expressions, and exposure to 77PDQ even at 0.01 μg/L decreased intestinal *hmp-2* expression (Fig. 2B). This suggested that the observed decrease in *hmp-2* expression might only induce a susceptibility to 77PDQ toxicity, and be not enough to cause altered intestinal barrier function in 77PDQ exposed nematodes. Different from this, only exposure to 10 μg/L IPPDQ decreased expressions of intestinal *pkc-3* and *acs-22* (Fig. 2B), which was consistent to the observed intestinal permeability after IPPDQ exposure. Exposure to 1 μg/L 6-PPDQ, 77PDQ, CPPDQ, DPPDQ, and DTPDQ and 10 μg/L of all the examined PPDQs decreased expressions of *hmp-2*, *erm-1*, *acs-22*, and/or *pkc-3* (Fig. 2B). Additionally, at 1 μg/L or 10 μg/L, PPDQs differentially affected *hmp-2*, *erm-1*, *acs-22*, and *pkc-3* expressions (Fig. 2B). These results provide an important basis at the molecular level for observed enhancement in intestinal barrier function after exposure to different PPDQs. In addition, different PPDQs may affect the intestinal barrier function through different molecular basis in nematodes.

For the intestinal toxicity, PPDQs not only caused disruption of intestinal barrier function, but also resulted in intestinal oxidative stress. Intestinal oxidative stress in PPDQs exposed nematodes was reflected by three aspects. The first aspect was to induce ROS production (Fig. 3). The second aspect was the increased MDA content and the decreased GSH content in nematodes exposed to different PPDQs (Fig. S3). MDA is a maker of oxidative stress, GSH is a maker of antioxidation in cells. The third aspect was to activate expressions of SOD-3::GFP and GST-4::GFP (Fig. 4). SOD-3 is a Mn-SOD, and GST-4 is a glutathione-S-transferase. Activation of SOD-3 and GST-4 indirectly reflects nematodes' response to oxidative stress induced by pollutants or stresses (Varão et al., 2021; Deng et al., 2021). Our previous study has indicated that 0.1–10 μg/L 6-PPDQ caused intestinal ROS production (Hua et al., 2023c). We further observed ROS production in nematodes exposed to 6-PPDQ (0.1–10 μg/L), 77PDQ (0.01–10 μg/L), CPPDQ (0.1–10 μg/L), DPPDQ (0.1–10 μg/L), DTPDQ (1–10 μg/L), and IPPDQ (1–10 μg/L) (Fig. 3). Meanwhile, the significant activation of SOD-3::GFP and GST-4::GFP was observed in nematodes exposed to 6-PPDQ (0.1–10 μg/L), 77PDQ (0.01–10 μg/L), CPPDQ (0.1–10 μg/L), DPPDQ (0.1–10 μg/L), DTPDQ (1–10 μg/L), and IPPDQ (1–10 μg/L) (Fig. 4). In the range of 0.01–10 μg/L, alterations in SOD-3::GFP and GST-4::GFP expressions were consistent with differences in induction of intestinal ROS production in PPDQs exposed nematodes. This implied that, in response to oxidative stress induced by PPDQs, SOD-3 and GST-4 would be activated to be against the corresponding toxicity of pollutants. Nevertheless, we found that the induction of ROS production was not completely consistent with enhanced intestinal permeability in PPDQs exposed nematodes. For example, no enhanced intestinal permeability was observed in 0.01 μg/L 77PDQ exposed nematodes (Fig. 2A); however, intestinal ROS production (Fig. 3) and activation of SOD-3::GFP and GST-4::GFP (Fig. 4) were detected in 0.01 μg/L 77PDQ exposed nematodes. This suggested that, on the one hand, induction of intestinal oxidative stress may contribute to formation of enhanced intestinal permeability in PPDQs exposed nematodes. On the other hand, at relatively low concentrations, intestinal oxidative stress induced by PPDQs may be not sufficient to disrupt intestinal barrier function.

Moreover, we provide two lines of evidence to indicate that decrease in *hmp-2*, *erm-1*, *acs-22*, and *pkc-3* expressions could potentially further strengthen PPDQs toxicity in inducing intestinal oxidative stress. Firstly, intestinal RNAi of *hmp-2*, *erm-1*, *acs-22*, and *pkc-3* resulted in a more pronounced induction of ROS production in nematodes exposed to 6-PPDQ, 77PDQ, CPPDQ, DPPDQ, DTPDQ, and/or IPPDQ (Fig. 5). Secondly, expressions of *hmp-2*, *erm-1*, *acs-22*, and *pkc-3* were significantly negative correlated with ROS production in nematodes exposed to 6-PPDQ, 77PDQ, CPPDQ, DPPDQ, DTPDQ, and/or IPPDQ (Fig. 6). Therefore, the decrease in expressions of intestinal *acs-22*, *erm-1*, *hmp-2*, and *pkc-3* provided an important mechanism of toxicity amplification in PPDQs exposed nematodes.

Among the examined PPDQs, the 6-PPDQ was first identified due to its role in inducing acute mortality of coho salmon (Tian et al., 2021). In this study, in the examined concentration range (0.01–10 μg/L), only exposure to 77PDQ could cause the lethality, and the obvious lethality was only detected in 10 μg/L 77PDQ exposed nematodes (Fig. 1B). The p-benzoquinone structure is a structural alert in organic chemicals, implying the potential for a wide range of adverse effects, such as acute cytotoxicity, immunotoxicity, teratogenicity and carcinogenicity (Bolton et al., 2000). Besides this, lipophilicity and molecular weight have

important effects on the toxicity of organic compounds (Yang et al., 2023). Octanol-Water Partition Coefficient (LogK_{oW}) is often used to predict the lipid solubility of chemicals. The LogK_{oW} (5.27) and molecular weight (334.26 g/mol) of 77PDQ are the highest among the examined PPDQs (Table S3). These may contribute to the formation of more severe 77PDQ toxicity in inducing lethality compared to other examined PPDQs. The IPPDQ was predicted to have the lowest lipid solubility (kow = 2.58) (Table S3), which was consistent with detected lowest intestinal toxicity of IPPDQ discussed above.

5. Conclusions

Together, we employed *C. elegans* as animal model to compare the intestinal toxicity among PPDQs (6-PPDQ, 77PDQ, CPPDQ, DPPDQ, DTPDQ, and IPPDQ). Different PPDQs caused enhanced intestinal permeability and affected expressions of some genes (*hmp-2*, *erm-1*, *acs-22*, and *pkc-3*) governing intestinal barrier function to different degrees. Meanwhile, the examined PPDQs caused intestinal ROS production and activation of SOD-3::GFP and GST-4::GFP to different degrees. Among examined PPDQs, 77PDQ showed more severe intestinal toxicity compared to other PPDQs. Moreover, genes of *hmp-2*, *erm-1*, *acs-22*, and *pkc-3* regulated PPDQs toxicity in inducing intestinal oxidative stress. Our results suggested the exposure risk of examined PPDQs in the range of ng/L or μg/L in causing intestinal toxicity in organisms.

CRediT authorship contribution statement

Yuxing Wang: Writing – original draft, Investigation. **Geyu Liang:** Supervision. **Jie Chao:** Supervision. **Dayong Wang:** Writing – review & editing, Supervision.

Declaration of competing interest

The authors declare that they have no known competing financial interests or personal relationships that could have appeared to influence the work reported in this paper.

Data availability

The data that has been used is confidential.

Acknowledgment

This study was supported by the grant from Shenzhen Basic Research Project (JCYJ20220530163605011).

Appendix A. Supplementary data

Supplementary data to this article can be found online at https://doi.org/10.1016/j.scitotenv.2024.172306.

References

Bolton, J.L., Trush, M.A., Penning, T.M., Dryhurst, G., Monks, T.J., 2000. Role of quinones in toxicology. Chem. Res. Toxicol. 13, 135–160.
Brenner, S., 1974. The genetics of *Caenorhabditis elegans*. Genetics 77, 71–94.
Cao, G., Wang, W., Zhang, J., Wu, P., Zhao, X., Yang, Z., Hu, D., Cai, Z., 2022. New evidence of rubber-derived quinones in water, air, and soil. Environ. Sci. Technol. 56, 4142–4150.
Cao, G., Wang, W., Zhang, J., Wu, P., Qiao, H., Li, H., Huang, G., Yang, Z., Cai, Z., 2023. Occurrence and fate of substituted p-phenylenediamine-derived quinones in Hong Kong wastewater treatment plants. Environ. Sci. Technol. 57, 15635–15643.
Chen, X., He, T., Yang, X., Gan, Y., Qing, X., Wang, J., Huang, Y., 2023. Analysis, environmental occurrence, fate and potential toxicity of tire wear compounds 6PPD and 6PPD-quinone. J. Hazard. Mater. 452, 131245.
Deng, Y., Du, H., Tang, M., Wang, Q., Huang, Q., He, Y., Cheng, F., Zhao, F., Wang, D., Xiao, G., 2021. Biosafety assessment of acinetobacter strains isolated from the three gorges reservoir region in nematode *Caenorhabditis elegans*. Sci. Rep. 11, 19721.
Deng, C., Huang, J., Qi, Y., Chen, D., Huang, W., 2022. Distribution patterns of rubber tire-related chemicals with particle size in road and indoor parking lot dust. Sci. Total Environ. 844, 157144.
Fang, L., Fang, C., Di, S., Yu, Y., Wang, C., Wang, X., Jin, Y., 2023. Oral exposure to tire rubber-derived contaminant 6PPD and 6PPD-quinone induce hepatotoxicity in mice. Sci. Total Environ. 869, 161836.
González-Manzano, S., González-Paramás, A.M., Delgado, L., Patianna, S., Surco-Laos, F., Dueñas, M., Santos-Buelga, C., 2012. Oxidative status of stressed *Caenorhabditis elegans* treated with epicatechin. J. Agric. Food Chem. 60, 8911–8916.
Grasse, N., Seiwert, B., Massei, R., Scholz, S., Fu, Q., Reemtsma, T., 2023. Uptake and biotransformation of the tire rubber-derived contaminants 6-PPD and 6-PPD quinone in the zebrafish embryo (*Danio rerio*). Environ. Sci. Technol. 57, 15598–15607.
He, W.-M., Gu, A.-H., Wang, D.-Y., 2023a. Four-week repeated exposure to tire-derived 6-PPD quinone causes multiple organ injury in male BALB/c mice. Sci. Total Environ. 894, 164842.
He, W.-M., Gu, A.-H., Wang, D.-Y., 2023b. Sulfonate-modified polystyrene nanoparticle at precited environmental concentrations induces transgenerational toxicity associated with increase in germline notch signal of *Caenorhabditis elegans*. Toxics 11, 511.
He, W.-M., Chao, J., Gu, A.-H., Wang, D.-Y., 2024. Evaluation of 6-PPD quinone toxicity on lung of male BALB/c mice by quantitative proteomics. Sci. Total Environ. 922, 171220.
Hua, X., Wang, D.-Y., 2023a. Tire-rubber related pollutant 6-PPD quinone: a review of its transformation, environmental distribution, bioavailability, and toxicity. J. Hazard. Mater. 459, 132265.
Hua, X., Wang, D.-Y., 2023b. Disruption of dopamine metabolism by exposure to 6-PPD quinone in *Caenorhabditis elegans*. Environ. Pollut. 337, 122649.
Hua, X., Wang, D.-Y., 2023c. Exposure to 6-PPD quinone at environmentally relevant concentrations inhibits both lifespan and healthspan in *C. elegans*. Environ. Sci. Technol. 57, 19295–19303.
Hua, X., Wang, D.-Y., 2024. Polyethylene nanoparticles at environmentally relevant concentrations enhances neurotoxicity and accumulation of 6-PPD quinone in *Caenorhabditis elegans*. Sci. Total Environ. 918, 170760.
Hua, X., Feng, X., Liang, G.-Y., Chao, J., Wang, D.-Y., 2023a. Exposure to 6-PPD quinone at environmentally relevant concentrations causes abnormal locomotion behaviors and neurodegeneration in *Caenorhabditis elegans*. Environ. Sci. Technol. 57, 4940–4950.
Hua, X., Feng, X., Liang, G.-Y., Chao, J., Wang, D.-Y., 2023b. Long-term exposure to 6-PPD quinone reduces reproductive capacity by enhancing germline apoptosis associated with activation of both DNA damage and cell corpse engulfment in *Caenorhabditis elegans*. J. Hazard. Mater. 454, 131495.
Hua, X., Feng, X., Liang, G.-Y., Chao, J., Wang, D.-Y., 2023c. Long-term exposure to tire-derived 6-PPD quinone causes intestinal toxicity by affecting functional state of intestinal barrier in *Caenorhabditis elegans*. Sci. Total Environ. 861, 160591.
Hua, X., Feng, X., Hua, Y.-S., Wang, D.-Y., 2023d. Paeoniflorin attenuates polystyrene nanoparticle-induced reduction in reproductive capacity and increase in germline apoptosis through suppressing DNA damage checkpoints in *Caenorhabditis elegans*. Sci. Total Environ. 871, 162189.
Hua, X., Cao, C., Zhang, L., Wang, D.-Y., 2023e. Activation of FGF signal in germline mediates transgenerational toxicity of polystyrene nanoparticles at predicted environmental concentrations in *Caenorhabditis elegans*. J. Hazard. Mater. 451, 131174.
Huang, W., Shi, Y., Huang, J., Deng, C., Tang, S., Liu, X., Chen, D., 2021. Occurrence of substituted p-phenylenediamine antioxidants in dusts. Environ. Sci. Technol. Lett. 8, 381–385.
Ji, J., Huang, J., Cao, N., Hao, X., Wu, Y., Ma, Y., An, D., Pang, S., Li, X., 2022a. Multiview behavior and neurotransmitter analysis of zebrafish dyskinesia induced by 6PPD and its metabolites. Sci. Total Environ. 838, 156013.
Ji, J., Li, C., Zhang, B., Wu, W., Wang, J., Zhu, J., Liu, D., Gao, R., Ma, Y., Pang, S., Li, X., 2022b. Exploration of emerging environmental pollutants 6PPD and 6PPDQ in honey and fish samples. Food Chem. 396, 133640.
Jin, R., Li, Y., Saito, Y., Wang, Z., Oanh Ta, T.K., Nguyen, V.L., Yang, J., Liu, M., Wu, Y., 2023. Amino accelerators and antioxidants in sediments from the Dong Nai River system, Vietnam: distribution and influential factors. Environ. Res. 227, 115712.
Johannessen, C., Metcalfe, C.D., 2022. The occurrence of tire wear compounds and their transformation products in municipal wastewater and drinking water treatment plants. Environ. Monit. Assess. 194, 731.
Liu, H.-L., Guo, D.-Q., Kong, Y., Rui, Q., Wang, D.-Y., 2019. Damage on functional state of intestinal barrier by microgravity stress in nematode *Caenorhabditis elegans*. Ecotoxicol. Environ. Saf. 183, 109554.
Liu, T., Zhuang, Z., Wang, D., 2023. Paeoniflorin mitigates high glucose-induced lifespan reduction by inhibiting insulin signaling in *Caenorhabditis elegans*. Front. Pharmacol. 14, 1202379.
Liu, Z.-Y., Hua, X., Zhao, Y., Bian, Q., Wang, D.-Y., 2024. Polyethylene nanoplastics cause reproductive toxicity associated with activation of both estrogenic hormone receptor NHR-14 and DNA damage checkpoints in *C. elegans*. Sci. Total Environ. 906, 167471.
Mahoney, H., da Silver Junior, F.C., Roberts, C., Schultz, M., Ji, X., Alcaraz, A.J., Montgomery, D., Selinger, S., Challis, J.K., Giesy, J.P., Weber, L., Janz, D., Wiseman, S., Hecker, M., Brinkmann, M., 2022. Exposure to the tire rubber-derived contaminant 6PPD-quinon causes mitochondrial dysfunction in vitro. Environ. Sci. Technol. Lett. 9, 765–771.
Mao, W., Jin, H., Guo, R., Chen, P., Zhong, S., Wu, X., 2024. Occurrence of p-phenylenediamine antioxidants in human urine. Sci. Total Environ. 914, 170045.
Maurer, L., Carmona, E., Machate, O., Schulze, T., Krauss, M., Brack, W., 2023. Contamination pattern and risk assessment of polar compounds in snow melt: an integrative proxy of road runoffs. Environ. Sci. Technol. 57, 4143–4152.

Monaghan, J., Jaeger, A., Jai, J.K., Tomlin, H., Atkinson, J.B., Brown, T.M., Gill, C.G., Krogh, E.T., 2023. Automated, high-throughput analysis of tire-derived p-phenylenediamine quinones (PPDQs) in water by online membrane sampling coupled to MS/MS. ACS ES&T Water 3, 3293–3304.

Qu, M., Xu, K.-N., Li, Y.-H., Wong, G., Wang, D.-Y., 2018. Using *acs-22* mutant *Caenorhabditis elegans* to detect the toxicity of nanopolystyrene particles. Sci. Total Environ. 643, 119–126.

Ren, M., Zhao, L., Ding, X., Krasteva, N., Rui, Q., Wang, D., 2018. Developmental basis for intestinal barrier against the toxicity of graphene oxide. Part. Fibre Toxicol. 15, 26.

Seiwert, B., Nihemaiti, M., Troussier, M., Weyrauch, S., Reemtsma, T., 2022. Abiotic oxidative transformation of 6-PPD and 6-PPD quinone from tires and occurrence of their products in snow from urban roads and in municipal wastewater. Water Res. 212, 118122.

Shao, Y.-T., Wang, Y.-X., Hua, X., Li, Y.-H., Wang, D.-Y., 2023. Polylactic acid microparticles in the range of μg/L reduce reproductive capacity by affecting the gonad development and the germline apoptosis in *Caenorhabditis elegans*. Chemosphere 336, 139193.

Shao, Y.-T., Hua, X., Li, Y.-H., Wang, D.-Y., 2024. Comparison of reproductive toxicity between pristine and aged polylactic acid microplastics in *Caenorhabditis elegans*. J. Hazard. Mater. 466, 133545.

Tang, M., Ding, G., Li, L., Xiao, G., Wang, D., 2023. Exposure to polystyrene nanoparticles at predicted environmental concentrations enhances toxic effects of *Acinetobacter johnsonii* AC15 infection on *Caenorhabditis elegans*. Ecotoxicol. Environ. Saf. 262, 115131.

Tian, Z., Zhao, H., Peter, K.T., Gonzalez, M., Wetzel, J., Wu, C., Hu, X., Prat, J., Mudrock, E., Hettinger, R., Cortina, A.E., Biswas, R.G., Kock, F.V.C., Soong, R., Jenne, A., Du, B., Hou, F., He, H., Lundeen, R., Gilbreath, A., Sutton, R., Scholz, N.L., Davis, J.W., Dodd, M.C., Simpson, A., McIntyre, J.K., Kolodziej, E.P., 2021. A ubiquitous tire rubber-derived chemical induces acute mortality in coho salmon. Science 371, 185–189.

Varão, A.M., Silva, J.D.S., Amaral, L.O., Aleixo, L.L.P., Onduras, A., Santos, C.S., Silva, L. P.D., Ribeiro, D.E., Filho, J.L.L., Bornhorst, J., Stiboller, M., Schwerdtle, T., Alves, L. C., Soares, F.A.A., Gubert, P., 2021. Toxic effects of thallium acetate by acute exposure to the nematode *C. elegans*. J. Trace Elem. Med. Biol. 68, 126848.

Varshney, S., Gora, A.H., Siriyappagouder, P., Kiron, V., Olsvik, P.A., 2022. Toxicological effects of 6PPD and 6PPD quinone in zebrafish larvae. J. Hazard. Mater. 424, 127623.

Wang, D.-Y., 2019. Target Organ Toxicology in *Caenorhabditis elegans*. Springer Nature Singapore Pte Ltd.

Wang, D.-Y., 2020. Exposure Toxicology in *Caenorhabditis elegans*. Springer Nature Singapore Pte Ltd.

Wang, D.-Y., 2022. Toxicology at Environmentally Relevant Concentrations in *Caenorhabditis elegans*. Springer Nature Singapore Pte Ltd.

Wang, Z., Xu, Z., Li, X., 2019. Impacts of methamphetamine and ketamine on *C. elegans*'s physiological functions at environmentally relevant concentrations and eco-risk assessment in surface waters. J. Hazard. Mater. 363, 268–276.

Wang, W., Cao, G., Zhang, J., Wu, P., Chen, Y., Chen, Z., Qi, Z., Li, R., Dong, C., Cai, Z., 2022. Beyond substituted p-phenylenediamine antioxidants: prevalence of their quinone derivatives in $PM_{2.5}$. Environ. Sci. Technol. 56, 10629–10637.

Wang, Y.-X., Hua, X., Wang, D.-Y., 2023a. Exposure to 6-PPD quinone enhances lipid accumulation through activating metabolic sensors of SBP-1 and MDT-15 in *Caenorhabditis elegans*. Environ. Pollut. 333, 121937.

Wang, Y.-X., Zhang, L., Yuan, X.-A., Wang, D.-Y., 2023b. Treatment with paeoniflorin increases lifespan of *Pseudomonas aeruginosa* infected *Caenorhabditis elegans* by inhibiting bacterial accumulation in intestinal lumen and biofilm formation. Front. Pharmacol. 14, 1114219.

Wang, Y.-X., Yuan, X.-A., Zhou, R., Bu, Y.-Q., Wang, D.-Y., 2023c. Combinational exposure to hydroxyatrazine increases neurotoxicity of polystyrene nanoparticles on *Caenorhabditis elegans*. Sci. Total Environ. 880, 163283.

Yang, L., Tian, R., Li, Z., Ma, X., Wang, H., Sun, W., 2023. Data driven toxicity assessment of organic chemicals against Gammarus species using QSAR approach. Chemosphere 328, 138433.

Yu, Y., Tan, S., Xie, D., Li, H., Chen, H., Dang, Y., Xiang, M., 2023. Photoaged microplastics induce neurotoxicity associated with damage to serotonergic, glutamatergic, dopaminergic, and GABAergic neuronal systems in *Caenorhabditis elegans*. Sci. Total Environ. 900, 165874.

Zeng, L., Li, Y., Sun, Y., Liu, L.Y., Shen, M., Du, B., 2023. Widespread occurrence and transport of p-phenylenediamines and their quinones in sediments across urban rivers, estuaries, coasts, and deep-sea regions. Environ. Sci. Technol. 57, 2393–2403.

Zhang, S., Gan, X., Shen, B., Jiang, J., Shen, H., Lei, Y., Liang, Q., Bai, C., Huang, C., Wu, W., Guo, Y., Song, Y., Chen, J., 2023a. 6PPD and its metabolite 6PPDQ induce different developmental toxicities and phenotypes in embryonic zebrafish. J. Hazard. Mater. 455, 131601.

Zhang, H., Huang, Z., Liu, Y., Hu, L., He, L., Liu, Y., Zhao, J., Ying, G., 2023b. Occurrence and risks of 23 tire additives and their transformation products in an urban water system. Environ. Int. 171, 107715.

Zhao, H.N., Hu, X., Gonzalez, M., Rideout, C.A., Hobby, G.C., Fisher, M.F., McCormick, C.J., Dodd, M.C., Kim, K.E., Tian, Z., Kolodziej, E.P., 2023. Screening p-phenylenediamine antioxidants, their transformation products, and industrial chemical additives in crumb rubber and elastomeric consumer products. Environ. Sci. Technol. 57, 2779–2791.

Zhu, J., Guo, R., Ren, F., Jiang, S., Jin, H., 2024a. Occurrence and partitioning of p-phenylenediamine antioxidants and their quinone derivatives in water and sediment. Sci. Total Environ. 914, 170046.

Zhu, J., Guo, R., Jiang, S., Wu, P., Jin, H., 2024b. Occurrence of p-phenylenediamine antioxidants (PPDs) and PPDs-derived quinones in indoor dust. Sci. Total Environ. 912, 169325.

Zhuang, Z., Liu, T., Liu, Z., Wang, D., 2024. Polystyrene nanoparticles strengthen high glucose toxicity associated with alteration in insulin signaling pathway in *C. elegans*. Ecotoxicol. Environ. Saf. 272, 116056.